

Received April 26, 2022, accepted May 16, 2022, date of publication May 20, 2022, date of current version May 27, 2022.

Digital Object Identifier 10.1109/ACCESS.2022.3176644

Adaptive Control With Unknown System Dynamics Estimator for Quadrotor Attitude Tracking

XIAOHUA ZHANG¹, JILIANG MU², AND CHAO JING²

¹School of Instrument and Electronics, North University of China, Taiyuan 030051, China

²School of Data Science and Technology, North University of China, Taiyuan 030051, China

Corresponding author: Xiaohua Zhang (zxh@nuc.edu.cn)

This work was supported by the National Key Research and Development Program of China under Grant 2019YFF0301802 and Grant 2019YFB2004802.

ABSTRACT This paper presents an adaptive control scheme via combining with an unknown system dynamics estimator (USDE) for attitude control of quadrotors subject to both parametric uncertainties and external disturbances. The presented controller is designed by effectively merging an adaptive control with an USDE via backstepping, where the extraneous uncertainties are addressed by USDE, and the adaptive law driven by tracking errors accounts for identifying unknown inertial moment constants. The unique characteristic is that a reinforced attitude controlling can be realized benefiting from the separate handling of parametric uncertainties and disturbances via an adaptive updating and a concise disturbance observation, significantly releasing the learning load of USDE and a high gain can be avoided in feedback loops. Meanwhile, Lyapunov analysis demonstrates that all error variables are uniformly ultimately bounded in the closed-loop system. Eventually, simulations substantiate the utility of suggested control strategy.


INDEX TERMS Unknown system dynamics estimator, adaptive control, quadrotor attitude control, backstepping.

I. INTRODUCTION

For the past few years, with the rapid development of electronic technology, quadrotors play a significant role in military and civilian fields. By virtue of their small size, low cost, strong mobility, quadrotors can perform diversified operations, such as aerial photography [1], target tracking [2], [3], rescue operations [4], and monitoring [6]. The attitude adjustment of quadrotors is the key factor to ensure the successful execution of above missions. However, the design of quadrotor controllers is encountered with tremendous challenges on account of unknown inertial moments and wind gusts. Therefore, it is necessary to exploit an attitude control scheme with strong adaptiveness for quadrotors to ensure the stability of attitude adjustment under uncertainties.

At present, a great deal of disturbance observers-based control literatures have been reported to resist the external disturbances and modeling uncertainties inherent in quadrotors, including neural network (NN) [7]–[10], extended state

observer (ESO) [13]–[16], and unknown system dynamics estimator (USDE) [17], [18]. Focusing on [8], a NN is utilized to estimate the parametric uncertainties for quadrotors. In [9], a NN with including of approximation components is proposed to estimate the modeling uncertainties for quadrotors. Moreover, [11] addresses the issue of adaptive intelligent asymptotic tracking control for a class of stochastic nonlinear systems with unknown control gains and full state constraints. In [12], the problem of adaptive output-feedback neural tracking control for a class of uncertain switched multiple-input multiple-output nonstrict-feedback nonlinear systems with time delays is investigated. However, an excessive tuning of neural weight updating is frequently involved in NN, making a remarkable increase in online computational load. To overcome this issue, a linear ESO with only one parameter to be determined is documented in [13], which can greatly reduce the tuning complexity encountered in NN. With the aid of ESO in [14], a sliding mode active disturbance rejection control scheme is proposed to handle trajectory tracking control problems for quadrotors. In [15], an ESO is utilized to improve the robustness and

The associate editor coordinating the review of this manuscript and approving it for publication was Zheng H. Zhu .

anti-disturbance ability for quadrotors. However, although ESO is capable of counteracting the external disturbances promptly and precisely, one should notice that a balance towards rapid convergence and peaking phenomenon should be cautiously treated [16]. To remedy this issue, based on the idea of invariant manifold and simple filtering operations on available states, a straightforward USDE with one filtering argument is developed to address lumped disturbances in an exponential decaying sense, permitting a simpler structure and a lower computational cost. Profiting from its advantages, sliding mode controllers integrated with an USDE are respectively practiced to achieve an enhanced tracking for servo mechanisms with unknown dynamics and modeling uncertainties [17] and quadrotor attitude adjustment [18]. And similar successful applications can be found in vehicle suspension control systems [19] and robotic systems [20]. However, various types of disturbances are simply regarded as a generalized term without discriminating parametric uncertainties and nonlinear disturbances, which increases the estimation burden of USDE especially in the event of heavy parametric perturbations. Thus, it is necessary to develop a compound estimation strategy to alleviate the learning load of USDE and pursue an improved tracking result.

Apart from disturbance observer-based control setting, a variety of nonlinear control schemes have been proposed for quadrotors. To name just a few, backstepping control [21], [22], sliding mode control [23]–[26], adaptive control [27], [28]. Among which, adaptive control is recognized as a preferred solution to overcome disturbance attenuation and retain closed-loop stability, wherein an adaptive parameter updating law is usually devised to approximate unknown nonlinearities written in a linear parameterized form. For instance, an adaptive command filtered backstepping [27] is proposed to stabilize the quadrotor systems. Similar approach can also be found in [29], where the problem of path following for quadrotors with unknown vehicle parameters, i.e., mass and moment of inertia and external disturbances is interviewed. Nevertheless, most of adaptive control schemes are integrated with robust mechanisms, such as robust integral sign error [30] to reinforce robustness and retain an asymptotic tracking, where a high gain in feedback loop is inevitably involved to attenuate the effect of disturbances within a small vicinity, leading to a great deal of energy consumption and control actions with severe chattering, which is unacceptable in implementations. It is worth mentioning that how to formulate a compound control policy to evade the need of high gain and reduce estimation load is still an open issue, which constitutes the major motivation.

Inspired by the previous statements, a straightforward viewpoint is to synthesize an adaptive control with a simple USDE to approximate parametric uncertainties and external disturbances separately for quadrotor attitude systems, allowing for a reinforced attitude tracking performance without relying on a high gain feedback and contributing to a lessened estimation burden compared with traditional

USDE [15], [16]. Additionally, through the deployment of adaptive control to update the unknown moment of inertia, yielding a more viable quadrotor control design against parameterized uncertainties. Furthermore, the effectiveness of the proposed method is proved by plentiful simulations in this paper. Lyapunov analysis demonstrates that the control system is stable. The primary innovations are summarized as

(1) Contrasting to the classical NN approximators [7]–[10], demanding a persistent exciting condition to guarantee the convergence of parameters while holding a complicated calculation process, by formulating a direct mapping between disturbance and the accessible states following filtering operations, a straightforward USDE is introduced to resist the external disturbances with an ensured error decaying and a reduced computational load. In addition, it can get rid of the peaking behaviors appearing in prevalent ESOs [13]–[16].

(2) Different from prevailing USDEs [17], [18] that treat all types of uncertainties as a total item, subject to an increased learning burden and a poor controlling behavior in the presence of severe parametric uncertainties, here parametric uncertainties and disturbances are separately dealt with via an adaptive updating and a disturbance observation, contributing to an improved tracking performances in terms of a minor attitude controlling deviation and a stronger anti-interference capability, while the learning load of USDE is released and the use of high gain feedback is avoided.

II. PROBLEM FORMULATION AND PRELIMINARIES

A. NOTATION

The following notations are listed for the convenience of clarification. $|\bullet|$ denotes the absolute value of a real number. $[\bullet]^T$ is the transpose of a vector and $\|\bullet\|$ refers to the Euclidean norm of a vector. $diag\{\bullet\}$ denotes a diagonal matrix. \mathbb{R} is a set of real numbers.

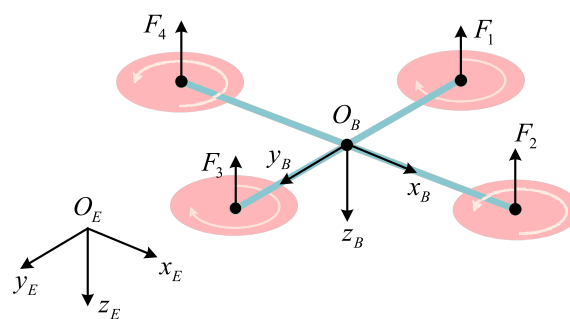


FIGURE 1. Physical structure of a quadrotor.

B. MODELLING OF QUADROTOR ATTITUDE SYSTEM

The physical structure of the quadrotor is shown as Fig. 1. The movement of quadrotors in space have six degrees of freedom, including roll, pitch, and yaw around its barycenter and the translational movement in three dimensional coordinates. The quadrotor can be regarded as an underactuated rigid body

with four actuating inputs. The lift force F_i ($i = 1, 2, 3, 4$) is supplied by four propellers, which is determined by the speed of four motors. Following [31], [32], the attitude dynamics of quadrotors can be represented by the following equations:

$$\begin{cases} \dot{\Theta} = \mathbf{R}\Omega \\ \mathbf{J}\dot{\Omega} = -\Omega \times \mathbf{J}\Omega + \tau + \mathbf{D} \end{cases} \quad (1)$$

where $\Theta = [\varphi, \theta, \psi]^T \in \mathbb{R}^{3 \times 1}$ represents the vector of Euler angles under earth-fixed frame $x_E - y_E - z_E$. $\Omega = [p, q, r]^T \in \mathbb{R}^{3 \times 1}$ stands for angular rates in body-fixed frame $x_B - y_B - z_B$. $\mathbf{J} = \text{diag}(J_x, J_y, J_z) \in \mathbb{R}^{3 \times 3}$ is an inertia moment matrix, which is unknown yet constant positive definite. $\tau = [\tau_1, \tau_2, \tau_3]^T \in \mathbb{R}^{3 \times 1}$ is deemed as the control input vector. $\mathbf{D} = [D_1, D_2, D_3]^T \in \mathbb{R}^{3 \times 1}$ represents the unmeasurable external disturbances. $\mathbf{R} \in \mathbb{R}^{3 \times 3}$ stands for the matrix relative to attitude angles, expressed by

$$\mathbf{R} = \begin{bmatrix} 1 & \sin \varphi \tan \theta & \cos \varphi \tan \theta \\ 0 & \cos \varphi & -\sin \varphi \\ 0 & \sin \varphi \sec \theta & \cos \varphi \sec \theta \end{bmatrix} \quad (2)$$

For the sake of description, we define $\mathbf{x}_1 = \Theta = [x_{11}, x_{12}, x_{13}]^T \in \mathbb{R}^{3 \times 1}$ and $\mathbf{x}_2 = \mathbf{R}\Omega = [x_{21}, x_{22}, x_{23}]^T \in \mathbb{R}^{3 \times 1}$. Based on this, attitude model (1) is rewritten as

$$\begin{cases} \dot{\mathbf{x}}_1 = \mathbf{x}_2 \\ \dot{\mathbf{x}}_2 = \underbrace{\dot{\mathbf{R}}\Omega + \mathbf{R}\mathbf{J}^{-1}(-\Omega \times \mathbf{J}\Omega + \mathbf{D})}_{\mathbf{G}_1} + \underbrace{\mathbf{R}(\mathbf{J}^{-1} - \mathbf{I})\tau + \tau}_{\mathbf{G}_2} \end{cases} \quad (3)$$

In quadrotor attitude dynamics (3), $\mathbf{G}_1 = [G_{11}, G_{12}, G_{13}]^T \in \mathbb{R}^{3 \times 1}$ refers to the vector of the lumped unknown disturbances. $\mathbf{G}_2 = [G_{21}, G_{22}, G_{23}]^T \in \mathbb{R}^{3 \times 1}$ represents the parametric uncertainties. Furtherly, for G_{2i} , there exists $G_{2i} = \theta^T \varphi_i$, where $\theta = [J_x^{-1} - 1, J_y^{-1} - 1, J_z^{-1} - 1]^T = [\theta_1, \theta_2, \theta_3]^T$ is an unknown vector to be identified, $\theta \in \{\theta | \theta_{\min} < \theta < \theta_{\max}\}$ with the lower and upper bounds being θ_{\min} and θ_{\max} respectively. $\varphi = \mathbf{R} \text{diag}(\tau_1, \tau_2, \tau_3) = [\varphi_1, \varphi_2, \varphi_3] \in \mathbb{R}^{3 \times 3}$ is a known regression matrix. Let $\hat{\theta}$ denote the estimate of θ and $\tilde{\theta} = \hat{\theta} - \theta$ stands for the estimation error. Thus, one has $\hat{G}_{2i} = \hat{\theta}^T \varphi_i$, $\tilde{G}_{2i} = \tilde{\theta}^T \varphi_i$, where $\hat{\theta} = [\hat{\theta}_1, \hat{\theta}_2, \hat{\theta}_3]^T \in \mathbb{R}^{3 \times 1}$, $\tilde{\theta} = [\tilde{\theta}_1, \tilde{\theta}_2, \tilde{\theta}_3]^T \in \mathbb{R}^{3 \times 1}$.

Assumption 1: The inertia of quadrotors is allowed to be piecewisely continuous but unknown.

Remark 1: Rotational inertia is a physical quantity indicating the rotational inertia of a rigid body, which is associated with the mass of the rigid body and the distribution of the mass relative to the rotating axis. For example, using a quadrotor to perform a payload transporting mission, when there is no payload, the mass of the system is equal to the mass of the vehicle, for the payload case, the mass of the system is the sum of the mass of the vehicle and the mass of

the payload. In both scenarios, we assume that the moment of inertia of the system is two different constants, and obviously they both remain within bounded boundaries.

A projection operator can be defined as

$$\text{Proj}_{\hat{\theta}_i}(\bullet) = \begin{cases} 0, & \hat{\theta}_i = \theta_{i\max} \text{ and } \bullet_i > 0 \\ 0, & \hat{\theta}_i = \theta_{i\min} \text{ and } \bullet_i < 0 \\ \bullet_i, & \text{otherwise} \end{cases} \quad (4)$$

where $i = 1, 2, 3$. Then, an adaptive parameter updating law is formulated as

$$\dot{\hat{\theta}} = \text{Proj}_{\hat{\theta}}(\Gamma\sigma), \theta_{\min} \leq \hat{\theta}(0) \leq \theta_{\max} \quad (5)$$

where $\Gamma > 0$ is an adaptive rate and $\sigma = [\sigma_1, \sigma_2, \sigma_3]^T$ is an adaptive function to be constructed. Profiting from the projection property, $\theta_{\min} \leq \hat{\theta} \leq \theta_{\max}$ always holds true. In addition, revisiting [33], σ satisfies:

$$\tilde{\theta}^T [\Gamma^{-1} \text{Proj}_{\hat{\theta}}(\Gamma\sigma) - \sigma] \leq 0 \quad (6)$$

Remark 2: For (3), unlike the regular anti-inference control solutions [11]–[16] that lump all dynamic uncertainties into a comprehensive item, here the equation of quadrotor model is rewritten into the integration of nonlinear uncertainties and a linear parametric form with a known regression matrix φ_i , facilitating the later control development under an observer and identification setting. The unique characteristic is that a reinforced attitude controlling can be implemented benefiting from the separate handling of parametric uncertainties and disturbances.

III. CONTROLLER DESIGN

In this section, the structure of the adaptive USDE attitude control strategy is introduced as elaborated in Fig.2. A disturbance observer, i.e., a concise USDE is constructed via straightforward filtering operations. Then, relying on an accurate compensation and an online parameter adaptive identification, a novel compound adaptive robust controller is integrated for quadrotor attitude regulation via backstepping.

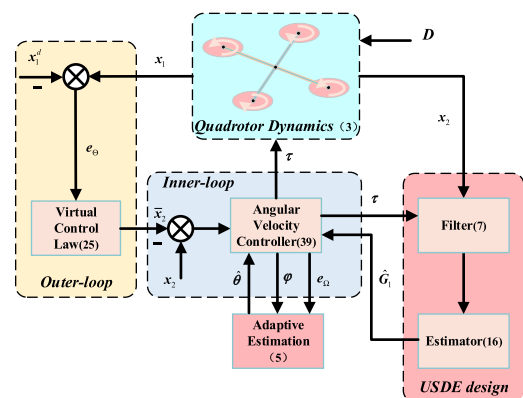


FIGURE 2. Illustration of control structure.

A. USDE DESIGN

For the measurable signal x_{2i} and τ_i , employing a low pass filtering algorithm $(\bullet)_f = (\bullet)/(ks + 1)$, indicated as

$$\begin{cases} k\dot{x}_{2i}^f + x_{2i}^f = x_{2i}, x_{2i}^f(0) = 0 \\ k\dot{G}_{2i}^f + G_{2i}^f = G_{2i}, G_{2i}^f(0) = 0 \\ k\dot{\tau}_i^f + \tau_i^f = \tau_i, \tau_i^f(0) = 0 \end{cases} \quad (7)$$

where $k > 0$ is a filtered constant.

Considering the principle of invariant manifold documented in [15], we obtain the following Lemma 1.

Lemma 1: Introducing an internal argument Z_i as

$$Z_i = (x_{2i} - x_{2i}^f)/k - \tau_i^f - G_{2i}^f - G_{1i} \quad (8)$$

where Z_i is asymptotic convergent, one has:

$$\lim_{k \rightarrow 0} \left[\lim_{t \rightarrow \infty} \left((x_{2i} - x_{2i}^f)/k - \tau_i^f - G_{2i}^f - G_{1i} \right) \right] = 0 \quad (9)$$

when $k \rightarrow 0$, it signifies that $(x_{2i} - x_{2i}^f)/k - \tau_i^f - G_{2i}^f - G_{1i} = 0$ is an invariant manifold.

Proof: Choose a Lyapunov candidate function as

$$V_{Z_i} = \sum_{i=1}^3 Z_i^2/2 \quad (10)$$

Taking the derivative of Z_i , it produces

$$\begin{aligned} \dot{Z}_i &= \sum_{i=1}^3 \left[(\dot{x}_{2i} - \dot{x}_{2i}^f)/k - \dot{\tau}_i^f - \dot{G}_{2i}^f - \dot{G}_{1i} \right] \\ &= \sum_{i=1}^3 \frac{1}{k} \left[\dot{x}_{2i} - (x_{2i} - x_{2i}^f)/k - (\tau_i - \tau_i^f) - (G_{2i} \right. \\ &\quad \left. - G_{2i}^f) - k\dot{G}_{1i} \right] \\ &= \sum_{i=1}^3 \left(-Z_i + k\dot{G}_{1i} \right)/k = \sum_{i=1}^3 \left(-Z_i/k - \dot{G}_{1i} \right) \end{aligned} \quad (11)$$

Based on (10), we have

$$\dot{V}_{Z_i} = \sum_{i=1}^3 Z_i \dot{Z}_i \quad (12)$$

Substituting (11) into (12) results in

$$\begin{aligned} \dot{V}_{Z_i} &= \sum_{i=1}^3 Z_i \dot{Z}_i = \sum_{i=1}^3 Z_i \left(-Z_i/k - \dot{G}_{1i} \right) \\ &= \sum_{i=1}^3 \left(-Z_i^2/k - Z_i \dot{G}_{1i} \right) \end{aligned} \quad (13)$$

On the basis of the Young's inequality, it yields

$$Z_i \dot{G}_{1i} \leq \frac{Z_i^2}{2k} + \frac{k\dot{G}_{1i}^2}{2} \quad (14)$$

Then (14) is reconstructed as follows:

$$\begin{aligned} \dot{V}_{Z_i} &\leq \sum_{i=1}^3 \left(-Z_i^2/k + Z_i^2/2k + k\dot{G}_{1i}^2/2 \right) \\ &= -V_{Z_i}/k + 3kg^2/2 \end{aligned} \quad (15)$$

where g is the upper limit of \dot{G}_{1i} . Integrating both sides of inequality (15) yields $V_{Z_i} \leq V_{Z_i}(0) e^{-t/k} + 3k^2g^2/2$, which means that Z_i is ultimately uniformly bounded (UUB). Then, it follows that $|Z_i| \leq \sqrt{2V_{Z_i}} \leq \sqrt{|Z_i(0)|^2 e^{-t/k} + 3k^2g^2}$. Hence, it reflects that $\lim_{k \rightarrow 0} \left[\lim_{t \rightarrow \infty} \left((x_{2i} - x_{2i}^f)/k - \tau_i^f - G_{2i}^f - G_{1i} \right) \right] = 0$ holds, indicating that $Z_i = 0$ is an invariant manifold.

Remark 3: Based on an ideal invariant manifold, the filtering calculation of USDE is constructed via adjusting a parameter k , greatly declining design complexity and computational cost compared with the neural approximate-based estimators [7]–[10]. Furthermore, it can be found that the convergence of the estimation error can be guaranteed by adjusting the filter parameters to a relatively small value, thus obtaining a more accurate estimation result than ESO [13]–[16].

As clarified from Lemma 1 that an explicit function between the disturbances and remaining system terms is given, then the estimate of nonlinear uncertainties existing in the inner loop is constructed based on Lemma 1 and filtering manipulation as

$$\hat{G}_{1i} = (x_{2i} - x_{2i}^f)/k - \tau_i^f - \hat{G}_{2i}^f \quad (16)$$

where \hat{G}_{1i} is the estimation of G_{1i} .

Theorem 1: For the developed USDE with an adaptive parameter estimation \hat{G}_{2i}^f , then the disturbance estimation error $\tilde{G}_{1i} = G_{1i} - \hat{G}_{1i}$, which is exponential convergence, maintaining $\lim_{k \rightarrow 0} \lim_{t \rightarrow \infty} \tilde{G}_{1i} \rightarrow 0$.

Proof: Taking the derivative of \tilde{G}_{1i} yields

$$\dot{\tilde{G}}_{1i} = \dot{G}_{1i} - \dot{\hat{G}}_{1i} = \dot{G}_{1i} - ((\dot{x}_{2i} - \dot{x}_{2i}^f)/k - \dot{\tau}_i^f - \dot{\hat{G}}_{2i}^f) \quad (17)$$

Notice that $\dot{\hat{G}}_{2i}^f = (\dot{G}_{2i} - \dot{\hat{G}}_{2i}^f)/k$. Then (17) can be rewritten as

$$\begin{aligned} \dot{\tilde{G}}_{1i} &= \dot{G}_{1i} - \left[\dot{x}_{2i} - (x_{2i} - x_{2i}^f)/k - (\tau_i - \tau_i^f) \right. \\ &\quad \left. - (\dot{G}_{2i} - \dot{\hat{G}}_{2i}^f) \right]/k \\ &= \dot{G}_{1i} - (\dot{x}_{2i} - \dot{G}_{1i} - \tau_i - \dot{G}_{2i})/k \\ &= \dot{G}_{1i} - (\tilde{G}_{1i} + \tilde{G}_{2i})/k \\ &= \dot{G}_{1i} - \tilde{G}_{1i}/k - \tilde{\theta}^T \varphi_i/k \end{aligned} \quad (18)$$

Considering the Lyapunov function as follows:

$$V_{G_{1i}} = \sum_{i=1}^3 \tilde{G}_{1i}^2/2 \quad (19)$$

Differentiating (19) and combining with Young's inequality, we have

$$\dot{V}_{G_{1i}} = \sum_{i=1}^3 \tilde{G}_{1i} \dot{\tilde{G}}_{1i} = \sum_{i=1}^3 \left(-\tilde{G}_{1i}^2/k + \tilde{G}_{1i} \dot{G}_{1i} - \tilde{G}_{1i} \tilde{\theta}^T \varphi_i/k \right) \quad (20)$$

Furthermore, $\dot{V}_{G_{ii}}$ is upper bounded by

$$\dot{V}_{G_{ii}} \leq \sum_{i=1}^3 \quad (21)$$

Adopting Young's inequality, and let $\bar{\varphi}_i = \varphi_i/k$, it yields

$$\begin{aligned} |\tilde{G}_{1i}|\dot{G}_{1i} &\leq \tilde{G}_{1i}^2/4k + kg^2 \\ |\tilde{G}_{1i}|\theta^T \bar{\varphi} &\leq \tilde{G}_{1i}^2/4k + k|\theta^T \bar{\varphi}|_{\max}^2 \end{aligned} \quad (22)$$

Substituting (22) into (21) has

$$\begin{aligned} \dot{V}_{G_{ii}} &\leq \sum_{i=1}^3 \left(-\tilde{G}_{1i}^2/2k + kg^2 + k|\theta^T \bar{\varphi}|_{\max}^2 \right) \\ &= -V_{G_{ii}}/k + \sum_{i=1}^3 k \left(g^2 + |\theta^T \bar{\varphi}|_{\max}^2 \right) \end{aligned} \quad (23)$$

By means of integrating both sides of inequality (23), one obtains $V_{G_{ii}} \leq V_{G_{ii}}(0) e^{-t/k} + 3k^2(g^2 + |\theta^T \bar{\varphi}|_{\max}^2)$, then

$$|\tilde{G}_{1i}| \leq \sqrt{2V_{G_{ii}}} \leq \sqrt{\tilde{G}_{1i}(0)^2 e^{-t/k} + 6k^2 \left(g^2 + |\theta^T \bar{\varphi}|_{\max}^2 \right)},$$

which indicates that \tilde{G}_{1i} is ultimately bounded and exponentially convergent towards the origin as $k \rightarrow 0$.

The proof is completed.

B. CONTROLLER DESIGN

According to the backstepping design principle, the quadrotor control problem can be divided into attitude level and angular rate level respectively. First, define the tracking deviation of attitude loop as $e_{\Theta} = x_1 - x_1^d$, where x_1^d is deemed as the attitude command. Next, taking the time derivative of e_{Θ} is derived by means of (3):

$$\dot{e}_{\Theta} = \dot{x}_1 - \dot{x}_1^d = x_2 - \dot{x}_1^d \quad (24)$$

A virtual control law is designed as:

$$\bar{x}_2 = -k_{\Theta} e_{\Theta} + \dot{x}_1^d \quad (25)$$

where \bar{x}_2 is velocity reference vector. k_{Θ} represents a non-negative control gain. Then define the tracking deviation of angular rate loop as $e_{\Omega} = x_2 - \bar{x}_2$, we have

$$\begin{aligned} \dot{e}_{\Theta} &= e_{\Omega} + \bar{x}_2 - \dot{x}_1^d = e_{\Omega} - k_{\Theta} e_{\Theta} + \dot{x}_1^d - \dot{x}_1^d \\ &= -k_{\Theta} e_{\Theta} + e_{\Omega} \end{aligned} \quad (26)$$

Differentiating e_{Ω} along the time, one has

$$\dot{e}_{\Omega} = \dot{x}_2 - \dot{\bar{x}}_2 \quad (27)$$

Substituting (3) into (27), we can obtain

$$\dot{e}_{\Omega} = G_1 + G_2 + \tau - \dot{\bar{x}}_2 \quad (28)$$

Utilizing the disturbance estimate offered by USDE and parameter identification via adaptive updating, the angular rate controller can be specified as

$$\tau = -k_{\Omega} e_{\Omega} + \dot{\bar{x}}_2 - \hat{G}_1 - e_{\Theta} - \hat{G}_2 \quad (29)$$

where $\hat{G}_1 = [\hat{G}_{11}, \hat{G}_{12}, \hat{G}_{13}]^T$, $\hat{G}_2 = [\hat{G}_{21}, \hat{G}_{22}, \hat{G}_{23}]^T$ and k_{Ω} represents a nonnegative control gain.

C. STABILITY ANALYSIS

Theorem 2: For a quadrotor attitude system (3) with adaptive parameter estimation law (5), USDE (16), attitude controller (25) and angular controller (29), where the adaptation function is designed as $\sigma = \varphi e_{\Omega}$. Then, all error signals involved in the closed-loop control framework can achieve UUB results.

Proof: The Lyapunov function for the tracking errors of attitude and angular rate is constructed as follows:

$$\begin{cases} V_{\Theta} = e_{\Theta}^T e_{\Theta} / 2 \\ V_{\Omega} = V_{\Theta} + e_{\Omega}^T e_{\Omega} / 2 \end{cases} \quad (30)$$

Considering (26), the differentiation of V_{Θ} is deduced as

$$\dot{V}_{\Theta} = e_{\Theta}^T \dot{e}_{\Theta} = e_{\Theta}^T (-k_{\Theta} e_{\Theta} + e_{\Omega}) = -k_{\Theta} e_{\Theta}^T e_{\Theta} + e_{\Theta}^T e_{\Omega} \quad (31)$$

Next, differentiating V_{Ω} , we have

$$\begin{aligned} \dot{V}_{\Omega} &= \dot{V}_{\Theta} + e_{\Omega}^T \dot{e}_{\Omega} = -k_{\Theta} e_{\Theta}^T e_{\Theta} + e_{\Theta}^T e_{\Omega} + e_{\Omega}^T \dot{e}_{\Omega} \\ &= -k_{\Theta} e_{\Theta}^T e_{\Theta} + e_{\Theta}^T e_{\Omega} + e_{\Omega}^T (G_1 + G_2 + \tau - \dot{\bar{x}}_2) \\ &= -k_{\Theta} e_{\Theta}^T e_{\Theta} + e_{\Theta}^T e_{\Omega} + e_{\Omega}^T (-k_{\Omega} e_{\Omega} - e_{\Theta} + \tilde{G}_1 + \tilde{G}_2) \\ &= -k_{\Theta} e_{\Theta}^T e_{\Theta} - k_{\Omega} e_{\Omega}^T e_{\Omega} + e_{\Omega}^T (\tilde{G}_1 + \tilde{G}_2) \end{aligned} \quad (32)$$

Considering the general Lyapunov function as follows:

$$V_a = \left(e_{\Theta}^T e_{\Theta} + e_{\Omega}^T e_{\Omega} + \tilde{G}_1^T \tilde{G}_1 + \tilde{\theta}^T \Gamma^{-1} \tilde{\theta} \right) / 2 \quad (33)$$

Combining with (18), (31) and (32), the time derivative of (33) is rewritten as

$$\begin{aligned} \dot{V}_a &= -k_{\Theta} e_{\Theta}^T e_{\Theta} - k_{\Omega} e_{\Omega}^T e_{\Omega} + e_{\Omega}^T (\tilde{G}_1 + \tilde{G}_2) \\ &\quad + \sum_{i=1}^3 \tilde{G}_{1i} (\dot{G}_{1i} - \tilde{G}_{1i}/k - \tilde{\theta}^T \varphi_i/k) + \tilde{\theta}^T \Gamma^{-1} \dot{\tilde{\theta}} \end{aligned} \quad (34)$$

According to Young's inequality and adaptive function property (6), (34) can be rewritten as

$$\begin{aligned} \dot{V}_a &\leq -k_{\Theta} e_{\Theta}^T e_{\Theta} - k_{\Omega} e_{\Omega}^T e_{\Omega} + e_{\Omega}^T e_{\Omega} / 2 + \tilde{G}_1^T \tilde{G}_1 / 2 + e_{\Omega}^T \varphi \tilde{\theta} \\ &\quad + \sum_{i=1}^3 \left(-\tilde{G}_{1i}^2 / 2k + kg^2 + k |\theta^T \bar{\varphi}_i|_{\max}^2 \right) + \tilde{\theta}^T \sigma \end{aligned} \quad (35)$$

Notice that $\sigma = \varphi e_{\Omega}$, (35) can be rewritten as

$$\begin{aligned} \dot{V}_a &\leq -k_{\Theta} e_{\Theta}^T e_{\Theta} - k_{\Omega} e_{\Omega}^T e_{\Omega} + e_{\Omega}^T e_{\Omega} / 2 + \tilde{G}_1^T \tilde{G}_1 / 2 \\ &\quad - \tilde{G}_1^T \tilde{G}_1 / 2k + 3kg^2 + 3k |\theta^T \bar{\varphi}_i|_{\max}^2 - \tilde{\theta}^T \tilde{\theta} + \|\theta\|_{\max}^2 \end{aligned} \quad (36)$$

Then we have

$$\begin{aligned} \dot{V}_a &\leq -k_{\Theta} e_{\Theta}^T e_{\Theta} - (k_{\Omega} - 1/2) e_{\Omega}^T e_{\Omega} - (1/2k - 1/2) \tilde{G}_1^T \tilde{G}_1 \\ &\quad - \tilde{\theta}^T \tilde{\theta} + 3kg^2 + 3k |\theta^T \bar{\varphi}_i|_{\max}^2 + \|\theta\|_{\max}^2 \end{aligned} \quad (37)$$

The control parameters are regulated such that $k_{\Theta} > 0$, $k_{\Omega} > 0.5$, $0 < k < 1$, \dot{V}_a can be designed as

$$\dot{V}_a \leq -KV_a + B \quad (38)$$

where $K = \min \{ \{2k_{\Theta}, 2k_{\Omega} - 1, (1 - k)/k, 2\Gamma\} > 0$ and $B = 3kg^2 + 3k \|\theta^T \bar{\varphi}_i\|_{\max}^2 + \|\theta_{\max}\|^2$.

Taking time integration of (38), then the following inequality can be reduced to

$$V_a(t) \leq V_a(0) e^{-Kt} + \frac{B}{K} \quad (39)$$

Hence, one can draw a conclusion that all error signals involved in the closed-loop control framework can achieve UUB results.

The proof is completed.

Remark 4: To facilitate the simulation of the proposed control algorithms, the related parameter tuning rules are summarized as follows:

(1) For USDE and adaptive parameter updating law, a reduced filter constant k contributes to an accurate estimate since it is related to observer bandwidth. As long as k is small enough, asymptotic convergence of the error can be achieved. And a bigger adaptive rate Γ helps to increase converge speed of identification.

(2) For attitude controller, larger k_{Θ} , k_{Ω} can obtain a more precise attitude tracking performance. However, overlarge k_{Θ} , k_{Ω} are inclined to yield transient fluctuations for control inputs, which will threaten the safety of quadrotors. Thus, it is necessary to regulate appropriate control gain k_{Θ} , k_{Ω} .

(3) All standard deviations of steady tracking and estimation errors are preserved within a sufficiently small size via selecting appropriate controller parameters, as elaborated in the following simulations.

IV. SIMULATION RESULTS

In this numerical simulation, plenty of simulation results are given in the MATLAB/SIMULINK environment with a sampling frequency of 1000Hz to verify the effectiveness of the proposed adaptive USDE controller. The physical parameters for quadrotor are set as follows: mass $m = 2kg$, gravitational acceleration $g = 9.8m/s^2$, the moments of inertia are supposed to be unknown and piecewisely continuous, taking the form of

$$J = \text{diag} \{ J_x, J_y, J_z \} = \begin{cases} \text{diag} \{ 0.16, 0.16, 0.32 \} \text{ kgm}^2, & 0 \leq t < 40 \\ \text{diag} \{ 0.5, 0.8, 0.6 \} \text{ kgm}^2, & 40 \leq t \leq 80 \end{cases} \quad (40)$$

External disturbances are selected as $\mathbf{D} = [0.2(\sin(t) + \sin(0.5t)), 0.2(\cos(0.5t) - \cos(0.8t)), 0.2(\sin(t)\sin(0.5t))]^T$. The initial state of attitude is $\Theta(0) = [0.5, 0.5, 0.005]^T \text{ rad}$. The initial value of the estimated parameter is $\hat{\theta}(0) = [6, 5.5, 3]^T$, and corresponding lower and upper bounds are $\theta_{\min} = [-5, -5, -5]^T$ and $\theta_{\max} = [10, 10, 10]^T$ respectively. Simulation parameters for the developed control algorithms are shown in TABLE.1.

A. EFFICACY VERIFICATION

Simulation results are displayed in Figs.3-10. Figs.3-4 clearly depicts that attitude profiles can precisely approximate to the

TABLE 1. Parameters for the control strategy.

Section	Values
USDE	$k = 0.01$
Adaptive attitude controller	$\Gamma = 25, k_{\Theta} = 5, k_{\Omega} = 10$

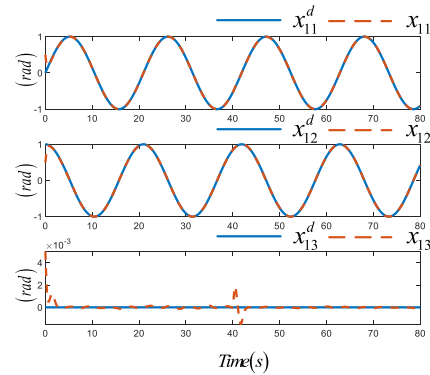


FIGURE 3. Attitude tracking curves.

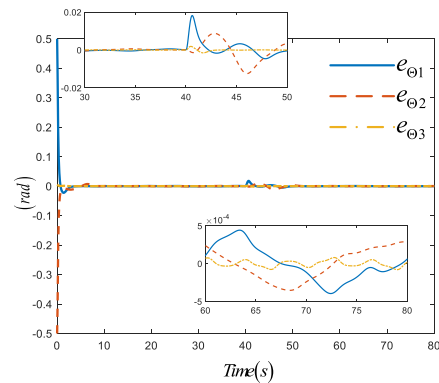


FIGURE 4. Attitude tracking errors.

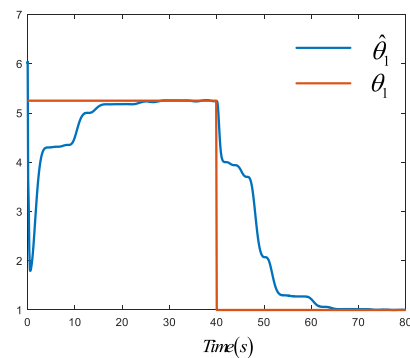


FIGURE 5. Estimated moment of inertia for θ_1 .

prescribed references with a sufficiently small tracking deviations despite of various uncertainties considered in quadrotor systems, note that during the time moment that inertia moment varies, the tracking error of yaw channel fluctuates a bit but soon converges to the origin, which is mainly profited

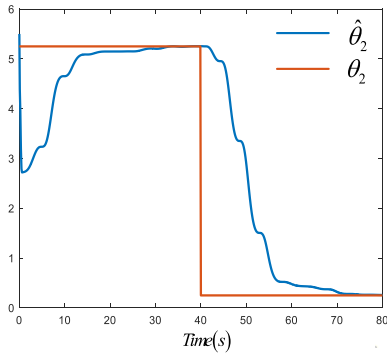


FIGURE 6. Estimated moment of inertia for θ_2 .

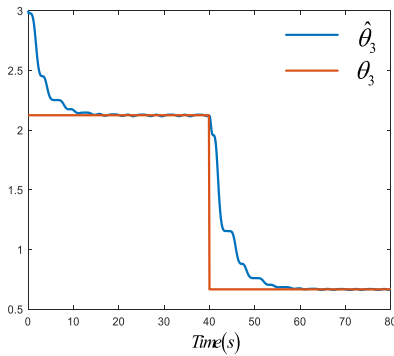


FIGURE 7. Estimated moment of inertia for θ_3 .

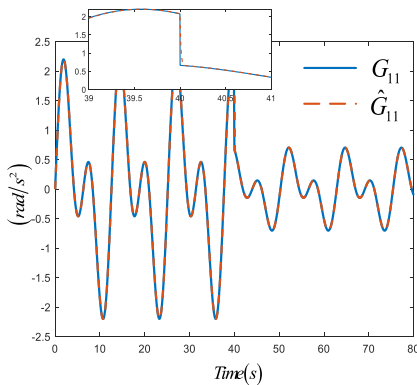


FIGURE 8. Disturbance G_{11} estimated by USDE.

from the deployment of adaptive parameter updating to capture the variation of unknown inertia moments online and the use of USDE to accurately accommodate the remaining disturbances in a feedforward way, as reflected from Figs.5-10. Additionally, as the parameter estimates approach to real values, the magnitude of unknown disturbances to be estimated is remarkably declined when time passes 40s, delivering a lessened learning burden for USDE and a high gain in control feedback loop can be avoided, which further validates the superiority of integrating parameter identification with disturbance observer to jointly resist system inferences.

To further illuminate the variation of different adaptive updating rates on parameter identification process, a group

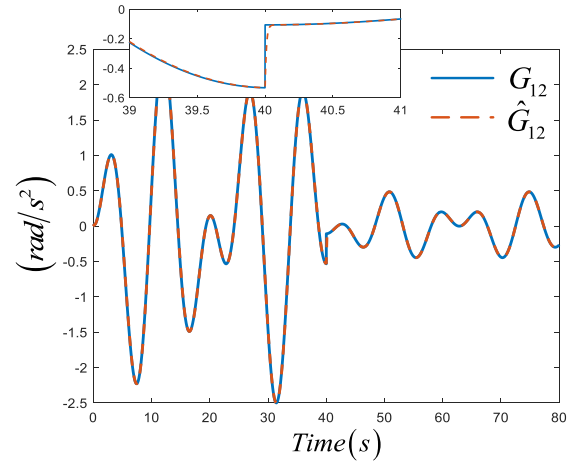


FIGURE 9. Disturbance G_{12} estimated by USDE.

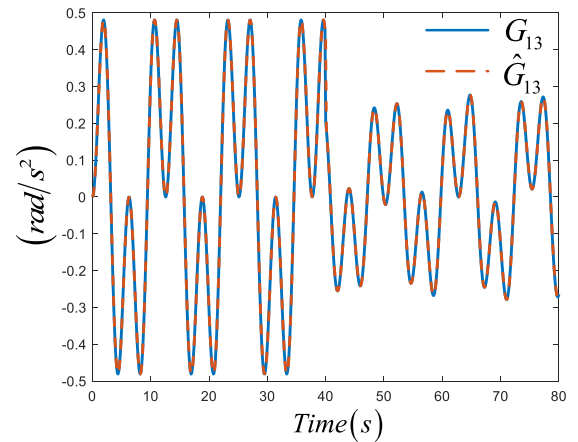


FIGURE 10. Disturbance G_{13} estimated by USDE.

of simulation comparisons with $\Gamma = 5, \Gamma = 15, \Gamma = 25$ are implemented respectively. As clearly observed from Fig.11, a faster approximation towards expected values can be achieved using a larger adaptive rate, contributing to a reinforced transient performance, but it should be stressed that an excessive adaptive gain tends to make the control inputs with more chattering, thus a tradeoff is suggested to be select with respect to smooth control actions and transient convergences.

B. COMPARISON WITH ADAPTIVE CONTROL [35] AND USDE-BASED CONTROL [18]

To further illustrate the merits of integrating adaptive parameter learning mechanism and disturbance compensation principle, here we compare the suggested algorithm with adaptive control [35] and USDE-based control [18]. To be specific, for adaptive control, parametric uncertainties are addressed by online parameter identification, while for the USDE-based control, all disturbances are roughly estimated by USDE. To retain a fair comparison, similar values of control parameters are chosen, in addition, the performances of considered

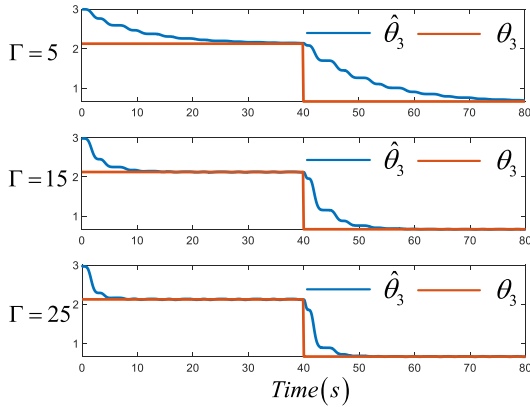


FIGURE 11. Parameter identification process using different adaptive rates.

TABLE 2. Comparison between adaptive control [35] and USDE-based control [18].

Section	RMSE (rad)		
	roll	pitch	yaw
Suggested method	1.1784	1.2365	0.0188
Adaptive control	1.2838	1.3069	0.2401
USDE-based control	1.2362	1.2866	0.0906

strategies are evaluated by root mean square error (RMSE) σ_e , calculated by:

$$\sigma_e = \sqrt{\sum_{k=1}^n [|e_{1i}(k)| - \mu_e]^2 / n} \quad (41)$$

where e_{1i} stands for attitude controlling deviation for each channel. μ_e represents the average value of errors. n is the sample size.

Table.2 summarizes RMSE of attitude tracking errors for different control algorithms. One can demonstrate from Table.2 that the developed compound control obtains the best control performance with the smallest RMSE, showing a great superiority in dealing with various kinds of uncertainties, as seen from Figs. 12-15. Conversely, for the other methods, it exhibits a relatively poor tracking capability in the presence of different uncertainties, further validating the advantages of synthesizing two different working mechanisms, i.e., parameter updating and disturbance observation.

C. COMPARATIVE STUDIES WITH ESO [36] AND RBFNN [37]

To reveal the validity of USDE in obtaining an improved estimation and control index, a series of simulation results are made with ESO [36] and RBFNN [37]. To guarantee a fair comparison, $\mathbf{G}_1, \mathbf{G}_2$ are treated as a total disturbance to be estimated by the considered estimators, while basic attitude controller remain the same. Following this line, the ideal invariant manifold establishes a mapping between filtering states $\mathbf{x}_{2i}^f, \tau_i^f$ and unknown system dynamics $\mathbf{D}_w = \mathbf{G}_1 + \mathbf{G}_2$, thus USDE is revised as

$$\hat{\mathbf{D}}_w = (\mathbf{x}_{2i} - \mathbf{x}_{2i}^f) / k - \tau_i^f \quad (42)$$

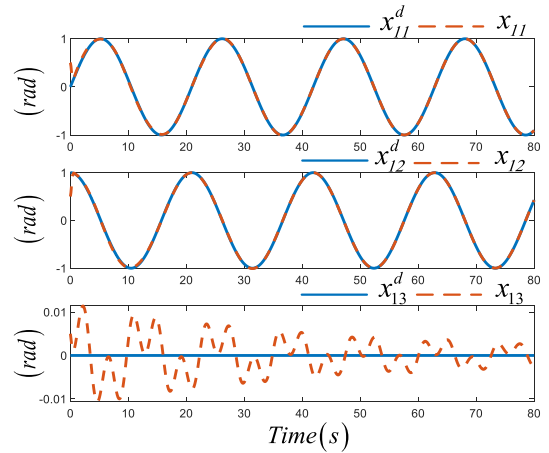


FIGURE 12. Attitude tracking curves of adaptive control [36].

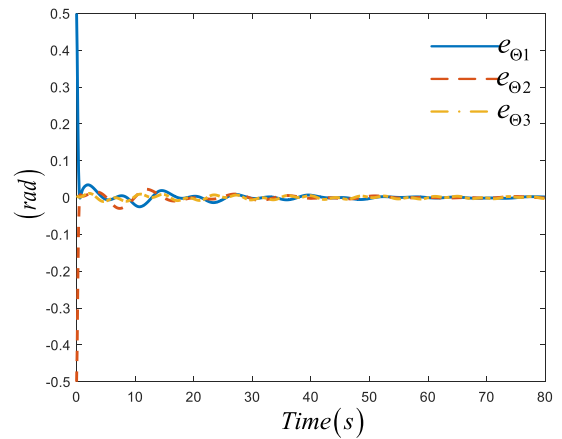


FIGURE 13. Attitude tracking errors of adaptive control [36].

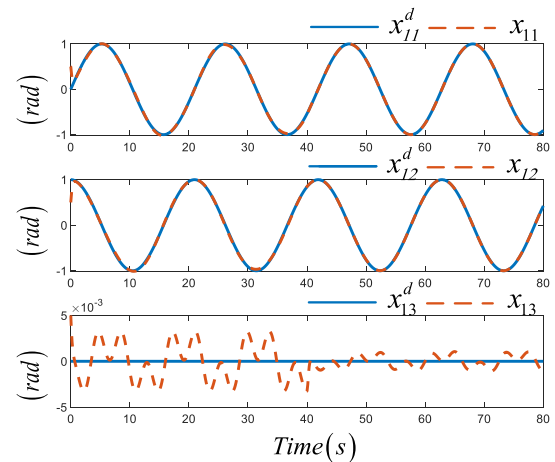


FIGURE 14. Attitude tracking curves of USDE-based control [18].

For ESO, according to [36], a second-order ESO is formulated as

$$\begin{cases} \dot{\hat{\mathbf{x}}}_2 = \hat{\mathbf{D}}_w + 2\omega_0(\mathbf{x}_2 - \hat{\mathbf{x}}_2) + \boldsymbol{\tau} \\ \dot{\hat{\mathbf{D}}}_w = \omega_0^2(\mathbf{x}_2 - \hat{\mathbf{x}}_2) \end{cases} \quad (43)$$

where $\omega_0 > 0$ is the observer gain, given as 100.

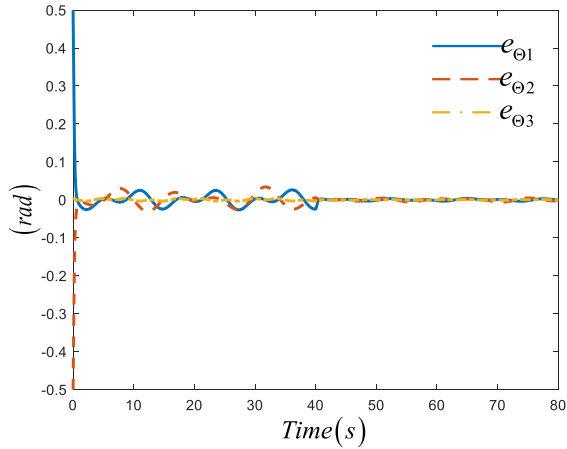


FIGURE 15. Attitude tracking errors of USDE-based control [18].

For RBFNN, unknown system dynamics is constructed as follows:

$$\hat{D}_i(\Phi_i) = w^T \zeta(\Phi_i), \quad i = \varphi, \theta, \psi \quad (44)$$

where $\Phi_i = [\tau_i, x_{2i}]^T$ represents input vector. $w \in \mathbb{R}^L$ is the devised weight with node number being L , which is chosen as 9. $\zeta(\Phi_i) = [\zeta_1, \zeta_2, \dots, \zeta_L]^T$ is written as

$$\zeta_j(\Phi_i) = \exp \left[-\|\Phi_i - \delta\|/2b_j^2 \right], \quad j = 1, 2, \dots, L \quad (45)$$

where δ is selected as $[0, 0]^T$. $b_j = 70$ is the width.

Table.3 lists the quantitative result of the mentioned methods, it is shown that owing to bounded estimation errors endowed by ESO and RBFNN, the contrastive methods are inferior to the suggested method with an exponential decaying ability regarding USDE, which demonstrates the correctness of Theorem 1. Above all, extensive outcomes substantiate the efficiency of suggested algorithm in enhancing robustness and tracking performances for quadrotor tracking.

TABLE 3. Performance comparison with ESO-based control [36] and RBFNN-based control [37].

Section	RMSE (rad)		
	roll	pitch	yaw
ESO-based control	1.0877	1.6745	0.0276
RBFNN-based control	1.1871	1.1888	0.0530

V. CONCLUSION

In this paper, an adaptive control scheme via combining with an USDE for attitude control of quadrotors subject to both parametric uncertainties and external disturbances is considered. In the designed controller, a parameter adaptation law and an USDE are developed and effectively merged to address uncertainties of inertial moment and remaining disturbances separately. By merging different working mechanisms, the proposed control scheme can retain the advantages of both

methods, meanwhile eliminating their performance limitations. Plenty of comparative results are acquired to verify the robustness of the constructed controller.

Further work will focus on introducing some intelligent learning techniques with suggested control to improve the adaptiveness of quadrotor under diversified operational environments.

REFERENCES

- [1] C.-L. Hwang, H.-M. Wu, and J.-Y. Lai, "On-line obstacle detection, avoidance, and mapping of an outdoor quadrotor using EKF-based fuzzy tracking incremental control," *IEEE Access*, vol. 7, pp. 160203–160216, 2019.
- [2] Y. Liu, Q. Wang, H. Hu, and Y. He, "A novel real-time moving target tracking and path planning system for a quadrotor UAV in unknown unstructured outdoor scenes," *IEEE Trans. Syst., Man, Cybern., Syst.*, vol. 49, no. 11, pp. 2362–2372, Nov. 2019.
- [3] A. Altan and R. Hacıoğlu, "Model predictive control of three-axis gimbal system mounted on UAV for real-time target tracking under external disturbances," *Mech. Syst. Signal Process.*, vol. 138, Apr. 2020, Art. no. 106548.
- [4] X. Yue, X. Shao, and W. Zhang, "Elliptical encircling of quadrotors for a dynamic target subject to aperiodic signals updating," *IEEE Trans. Intell. Transp. Syst.*, early access, Nov. 24, 2021, doi: 10.1109/TITS.2021.3127722.
- [5] L. Tang, H. S. Wang, Z. Liu, and Y. Wang, "A real-time quadrotor trajectory planning framework based on B-spline and nonuniform kinodynamic search," *J. Field Robot.*, vol. 38, no. 3, pp. 452–475, May 2021.
- [6] W. H. Cheng and C. S. Yuan, "Using a micro sampler on a drone to extract organic vapors—A case study of monitoring industrial pollution," *Aerosol Air Qual. Res.*, vol. 21, no. 2, Feb. 2021, Art. no. 200359.
- [7] L. Guettal, H. E. Glida, and A. Chelih, "Adaptive fuzzy-neural network based decentralized backstepping controller for attitude control of quadrotor helicopter," in *Proc. 1st Int. Conf. Commun., Control Syst. Signal Process. (CCSSP)*, May 2020, pp. 394–399.
- [8] Y. C. Ouyang, L. Xue, L. Dong, and C. Y. Sun, "Neural network-based finite-time distributed formation-containment control of two-layer quadrotor UAVs," *IEEE Trans. Syst., Man, Cybern., Syst.*, early access, Aug. 25, 2021, doi: 10.1109/TSMC.2021.3103013.
- [9] B. Xian, C. Diao, B. Zhao, and Y. Zhang, "Nonlinear robust output feedback tracking control of a quadrotor UAV using quaternion representation," *Nonlinear Dyn.*, vol. 79, no. 4, pp. 2735–2752, Mar. 2015.
- [10] Z. Chen, F. Huang, W. Sun, J. Gu, and B. Yao, "RBF-neural-network-based adaptive robust control for nonlinear bilateral teleoperation manipulators with uncertainty and time delay," *IEEE/ASME Trans. Mechatronics*, vol. 25, no. 2, pp. 906–918, Apr. 2020.
- [11] W. Su, B. Niu, H. Wang, and W. Qi, "Adaptive neural network asymptotic tracking control for a class of stochastic nonlinear systems with unknown control gains and full state constraints," *Int. J. Adapt. Control Signal Process.*, vol. 35, no. 10, pp. 2007–2024, Oct. 2021.
- [12] J. Kong, B. Niu, Z. Wang, P. Zhao, and W. Qi, "Adaptive output-feedback neural tracking control for uncertain switched MIMO nonlinear systems with time delays," *Int. J. Syst. Sci.*, vol. 52, no. 13, pp. 2813–2830, Oct. 2021.
- [13] J. Liu, W. Gai, J. Zhang, and Y. Li, "Nonlinear adaptive backstepping with ESO for the quadrotor trajectory tracking control in the multiple disturbances," *Int. J. Control, Autom. Syst.*, vol. 17, no. 11, pp. 2754–2768, Nov. 2019.
- [14] Y. Wu, J. Sun, and Y. Yu, "Trajectory tracking control of a quadrotor UAV under external disturbances based on linear ADRC," in *Proc. 31st Youth Academic Annu. Conf. Chin. Assoc. Autom. (YAC)*, Nov. 2016, pp. 13–18.
- [15] X. Shao, L. Xu, and W. Zhang, "Quantized control capable of appointed-time performances for quadrotor attitude tracking: Experimental validation," *IEEE Trans. Ind. Electron.*, vol. 69, no. 5, pp. 5100–5110, May 2022.
- [16] B. Wang, Y. Shen, and Y. Zhang, "Active fault-tolerant control for a quadrotor helicopter against actuator faults and model uncertainties," *Aerosp. Sci. Technol.*, vol. 99, Apr. 2020, Art. no. 105745.
- [17] S. Wang, L. Tao, Q. Chen, J. Na, and X. Ren, "USDE-based sliding mode control for servo mechanisms with unknown system dynamics," *IEEE/ASME Trans. Mechatronics*, vol. 25, no. 2, pp. 1056–1066, Apr. 2020.

- [18] L. Xu, X. Shao, and W. Zhang, "USDE-based continuous sliding mode control for quadrotor attitude regulation: Method and application," *IEEE Access*, vol. 9, pp. 64153–64164, 2021.
- [19] Y. Huang, J. Wu, J. Na, S. Han, and G. Gao, "Unknown system dynamics estimator for active vehicle suspension control systems with time-varying delay," *IEEE Trans. Cybern.*, early access, May 7, 2021, doi: [10.1109/TCYB.2021.3063225](https://doi.org/10.1109/TCYB.2021.3063225).
- [20] J. Na, B. Jing, Y. Huang, G. Gao, and C. Zhang, "Unknown system dynamics estimator for motion control of nonlinear robotic systems," *IEEE Trans. Ind. Electron.*, vol. 67, no. 5, pp. 3850–3859, May 2020.
- [21] M. Sharma and I. Kar, "Control of a quadrotor with network induced time delay," *ISA Trans.*, vol. 111, pp. 132–143, May 2021.
- [22] X. Wang, Y. Chen, Y. Lu, and X. Li, "Dynamic surface method-based adaptive backstepping control for the permanent magnet synchronous motor on parameter identification," *Proc. Inst. Mech. Eng., I, J. Syst. Control Eng.*, vol. 233, no. 9, pp. 1172–1181, Oct. 2019.
- [23] N. Ahmed and M. Chen, "Sliding mode control for quadrotor with disturbance observer," *Adv. Mech. Eng.*, vol. 10, no. 7, Jul. 2018, Art. no. 168781401878233.
- [24] Y. Chen, P. Zhu, P. Zhang, M. Li, Z. Wan, and W. Zhang, "Hybrid sliding-mode position-tracking control for servo system with external disturbance," *IEEE J. Emerg. Sel. Topics Power Electron.*, vol. 9, no. 5, pp. 5478–5488, Oct. 2021.
- [25] X. Shao, Y. Shi, and W. Zhang, "Fault-tolerant quantized control for flexible air-breathing hypersonic vehicles with appointed-time tracking performances," *IEEE Trans. Aerosp. Electron. Syst.*, vol. 57, no. 2, pp. 1261–1273, Apr. 2021.
- [26] X. Shao, Y. Shi, and W. Zhang, "Input-and-Measurement event-triggered output-feedback chattering reduction control for MEMS gyroscopes," *IEEE Trans. Syst., Man, Cybern., Syst.*, early access, Dec. 2, 2021, doi: [10.1109/TSMC.2021.3129275](https://doi.org/10.1109/TSMC.2021.3129275).
- [27] T. X. Dinh and K. K. Ahn, "Adaptive tracking control of a quadrotor unmanned vehicle," *Int. J. Precis. Eng. Manuf.*, vol. 18, no. 2, pp. 163–173, 2017.
- [28] J. Fei and Z. Feng, "Adaptive super-twisting sliding mode control for micro gyroscope based on double loop fuzzy neural network structure," *Int. J. Mach. Learn. Cybern.*, vol. 12, no. 3, pp. 611–624, Mar. 2021.
- [29] W. Xie, D. Cabecinhas, R. Cunha, and C. Silvestre, "Adaptive backstepping control of a quadcopter with uncertain vehicle mass, moment of inertia, and disturbances," *IEEE Trans. Ind. Electron.*, vol. 69, no. 1, pp. 549–559, Jan. 2022.
- [30] J. Yao, Z. Jiao, and D. Ma, "RISE-based precision motion control of DC motors with continuous friction compensation," *IEEE Trans. Ind. Electron.*, vol. 61, no. 12, pp. 7067–7075, Dec. 2014.
- [31] X. Wang and B. Shirinzadeh, "Nonlinear augmented observer design and application to quadrotor aircraft," *Nonlinear Dyn.*, vol. 80, no. 3, pp. 1463–1481, May 2015.
- [32] F. Kendoul, "Nonlinear hierarchical flight controller for unmanned rotorcraft: Design, stability, and experiments," *J. Guid., Control, Dyn.*, vol. 32, no. 6, pp. 1954–1958, Nov. 2009.
- [33] J. Yao and W. Deng, "Active disturbance rejection adaptive control of hydraulic servo systems," *IEEE Trans. Ind. Electron.*, vol. 64, no. 10, pp. 8023–8032, Oct. 2017.
- [34] H. Razmi, "Adaptive neural network based sliding mode altitude control for a quadrotor UAV," *J. Central South Univ.*, vol. 25, no. 11, pp. 2654–2663, Dec. 2018.
- [35] T. Huang, D. Huang, Z. Wang, X. Dai, and A. Shah, "Generic adaptive sliding mode control for a quadrotor UAV system subject to severe parametric uncertainties and fully unknown external disturbance," *Int. J. Control, Autom. Syst.*, vol. 19, no. 2, pp. 698–711, Feb. 2021.
- [36] R. Zhou, C. Fu, and W. Tan, "Implementation of linear controllers via active disturbance rejection control structure," *IEEE Trans. Ind. Electron.*, vol. 68, no. 7, pp. 6217–6226, Jul. 2021.
- [37] C. L. P. Chen, G.-X. Wen, Y.-J. Liu, and F.-Y. Wang, "Adaptive consensus control for a class of nonlinear multiagent time-delay systems using neural networks," *IEEE Trans. Neural Netw. Learn. Syst.*, vol. 25, no. 6, pp. 1217–1226, Jun. 2014.

...